JOURNAL OF MATERIALS SCIENCE 16 (1981) 1616–1626

# An investigation of the liquid impact properties of a GFRP radome material

M. J. MATTHEWSON, D. A. GORHAM*
*Physics and Chemistry of Solids, Cavendish Laboratory, Madingley Road, Cambridge, UK*

The damage caused by the impact of high velocity water jets (100 to 1200 m sec$^{-1}$) on GFRP specimens from a prototype Concorde radome has been investigated. The dependencies of the extent of various damage modes on the jet velocity, size and angle of impact have been studied in detail. The effect of multiple impacts has also been examined. The results are interpreted in terms of the fundamental deformation and failure mechanisms of a composite system. The results show that damage is sensitive to the size and velocity of the impacting jet and that more damage may occur for oblique impact than for normal impact. The liquid jets model impact by spherical drops and the conclusions are therefore relevant to the case of rain erosion.

## 1. Introduction

Composite materials have been extensively used as aircraft microwave radomes, possessing two properties required by such an application: they have a high strength-to-weight ratio while having sufficient fracture toughness to withstand normal operating conditions, and they can be transparent to microwaves. Composites have, however, poor resistance to high velocity impact compared with many other structural materials and this imposes a serious limiting factor when designing components for use on forward-facing exposed surfaces of aircraft which may fly through rain at high speeds. In practice, erosion damage may be greatly reduced by using very hard (e.g. ceramic, although ceramics are not generally suitable for large structures) or very soft (e.g. elastomeric) coatings, or by taking advantage of large sweepback.

This paper describes a detailed investigation of the high-velocity liquid impact properties of a particular material developed for the radome of the Concorde supersonic aircraft. The results obtained illustrate the dependence of damage on the velocity, size, obliqueness and number of liquid impacts.

The results, while being of use as "worst case" data on the Concorde radome, also outline basic principles which may be applied to the behaviour of other composite materials under various impact or erosive conditions: for example jet-engine compressor blades and high-speed turbine blades.

This study is intended to establish failure mechanisms which apply generally to the behaviour of a laminated composite structure and in particular to radomes of this type. The samples were not protectively coated in the manner used for Concorde or other radomes and are therefore not typical of the in-flight situation unless, of course, failure of the protective film has occurred. Under these unprotected conditions erosion effects can be very severe so it is worth noting that rain erosion has not exhibited itself as a problem on the Concorde aircraft.

## 2. Description of the radome

The radome is a one-piece cone (11° semi-conical angle) fabricated from a glass-fibre reinforced epoxy resin by B. Ae. Dynamics (Stevenage). Reinforcement consists of alternate layers of knitted (18 layers) and woven (17 layers) "E"-glass fabric. The outermost layer is knitted. The resin system is Araldite MY720+HY906 (100:110 pbw) with a cure of 72 h at 50° C followed by a post cure of 16 h at 100° C and 20 h at 150° C. The reinforcement content is 38% by weight and the

*Present address: The Faculty of Technology, The Open University, Walton Hall, Milton Keynes, UK.


0022–2461/81/061616–11$03.10/0 

overall thickness of the material is 9 mm. There is no gel-coat and fibre bundles of the top lamination are at the matrix–air interface.

## 3. Experimental procedure

High-velocity bodies of water were produced by the technique of Bowden and Brunton [1], in which a lead air-gun pellet is fired into the rear of a nozzle filled with water sealed in by a neoprene disc. The pellet and neoprene drive forward as a piston, extruding a short jet of water at high velocity from a narrow orifice at the front of the nozzle. The target is placed ~ 10 mm from the exit orifice. The pellet is accelerated by a gas-gun with a continuously variable firing pressure. Thus, the impact velocity is controlled over a range from 100 to 1200 m $sec^{-1}$. More information about the production and properties of the jets may be found in Field *et al.* [2].

The impact of these water jets is an accurate model for the more realistic situation of a moving solid impact on stationary liquid drops [2, 3]. The jet method is experimentally more convenient and more rapid in operation than firing the specimen at high velocity towards a suspended drop. Also the jet technique can simulate the impact of drops that are too large to be freely supported.

Three nozzle orifice sizes have been used in this investigation, with diameters of 0.8, 1.6 and 2.4 mm. Table I gives the jet head diameter at impact and the equivalent spherical drop diameter for these three nozzles. These data are valid over the velocity range of this work. The jets will be referred to by their head diameter. The equivalent drop diameters are very large; drops of this size form only a small proportion of a rain field. A study of large equivalent drops can, however, be justified in two ways. Firstly, the impact damage is dependent on the radius of curvature of the impacting face of the drop rather than the mean radius. Drops in free fall oscillate in shape between being oblate and prolate spheroids and so can have a large instantaneous radius of curvature. Also, both experimental [4] and theoretical [5] work has shown that a drop is deformed by passing through the air shock-wave preceding a supersonic body giving a large radius of curvature. Experimental work in this laboratory has shown that large drop sizes produce disproportionately more damage than smaller ones, and more damage than by repeated impacts by smaller drops of the same total volume. Thus, a few large or distorted drops encountered in the rain field cause most damage, which is then extended by the impact of smaller drops. These reasons justify taking a "worst case" attitude in this study.

TABLE I

| Nozzle exit orifice diameter (mm) | Jet head diameter (mm) | Equivalent drop diameter (mm) |
|---|---|---|
| 0.8 | 1.5 | 5 |
| 1.6 | 3.0 | 10 |
| 2.4 | 4.5 | 15 |

### 3.1. The impact process

When the head of the jet reaches the solid surface the water initially behaves compressibly, generating the "water-hammer" pressure given by $\rho CV$ (where $\rho$ is the liquid density, $C$ is the shock-wave velocity in the liquid and $V$ is the impact velocity). Compressible behaviour ceases when release waves from the free surface reach the centre of the liquid allowing it to jet sideways. The duration of the $\rho CV$ pressure is therefore given by $d/2C$ where $d$ is the diameter of the jet. Therefore, a short pulse of very high pressure is produced [1]. With a 700 m $sec^{-1}$, 3 mm diameter jet the impact pressure is ~ 1.5 GPa, (depending on the properties of the target), and lasts for ~ 1 $\mu$sec. This type of impulsive loading is substantially different from the general case of solid impact, in which contact durations are typically much longer. However, liquid impact is very similar to explosive loading and to the impact of very small solid projectiles.

Material damage under liquid impact arises from three principal mechanisms:

(1) Compressive and shear stresses under the contact area;

(2) Shearing action of the high velocity radial jetting which erodes surface discontinuities;

(3) Interactions of stress waves can cause damage far from the impact site, but can to some extent be controlled by the specimen dimensions.

These mechanisms do not depend upon the detailed shape of the impacting liquid which explains the similarity between the damage produced by spherical drops and the cylindrical jets.

## 4. Normal impact results

Fig. 1a shows the damage produced by a 3 mm jet impacting at normal incidence with a velocity of 815 m $sec^{-1}$. The photograph shows a central region, A, where the matrix has been chipped

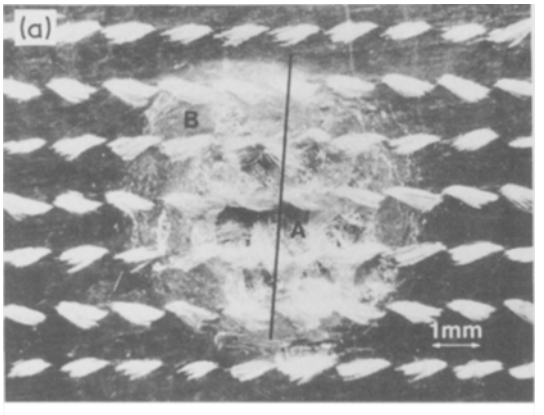


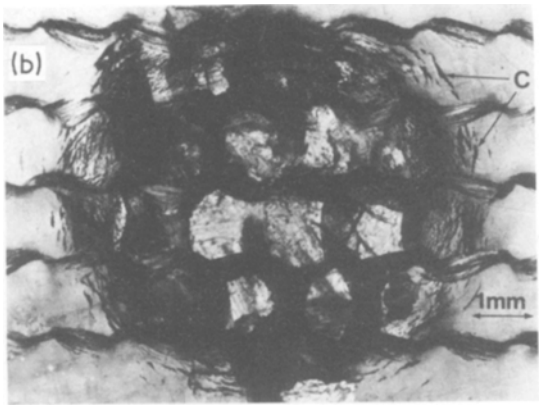


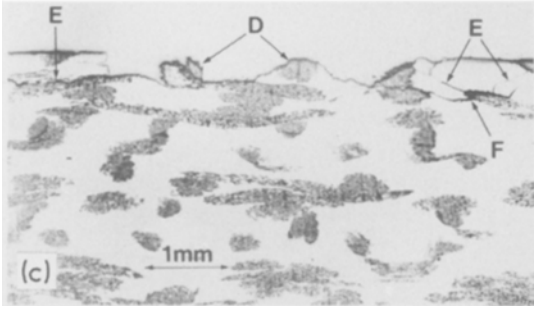


*Figure 1* Impact sites on the radome: (a) Damage due to impact by a 815 m sec$^{-1}$ 3 mm diameter jet at normal incidence; (b) same site as (a) but in transmitted illumination and (c) section through the damage site along the line shown in (a).

away exposing the essentially undamaged fibre bundles of the surface lamination; only a few individual fibres are fractured. This area is subjected to high compressive loading and failure modes are discussed by Gorham and Field, [6]. Surrounding this central area is a region, B, which is paler than the undamaged material because of light scattered by subsurface areas of debonding and interlaminar fracture. This region has approximately twice the area of the central region and extends well beyond the jet contact area. Fig. 1b is a photograph of the same site as Fig. 1a but transmitted illumination shows a large number of small circumferential cracks indicated by C. Similar cracks are observed around impact sites on brittle isotropic materials and are attributed to the passage of the intense Rayleigh surface stress-pulse formed by the impulsive loading [7].

Fig. 1c is a section taken through the same impact site along the line shown in Fig. 1a and shows interesting features. It can be seen that only the surface lamination is penetrated, leaving exposed fibre bundles, D. Around the area of visible surface damage is a network of cracks, E, whose fracture surfaces are widely separated. The surface above these cracks is therefore raised slightly which is not an artefact of the sample preparation but is observed on damage sites prior to sectioning. One area of matrix has been lifted to form a cavity, F. The region is severely damaged and a further impact would dislodge much of this loose material, dramatically increasing the visible surface damage.

Impact sites for 1.5 and 4.5 mm jets show similar damage features but the extents of the various damage modes differ due to size effects. The threshold velocity for damage increases with decreasing jet diameter (to be discussed later). The surface damage will depend upon the compressive stress produced by the impact, given approximately by $\rho CV$, and the lateral jetting velocity, both of which increase with impact velocity. Thus, considering impact just above the threshold for damage for the given jet diameter, the impact pressure and lateral jetting velocity are higher for smaller jets and so these produce greater penetration, but over a smaller area than larger jets. However, the impact duration increases in proportion to the jet diameter and smaller jets have shorter impact durations and plate bending, and hence, interlaminar failure is less extensive than for larger jets, Conversely, larger jets produce less surface damage over a larger area but do produce larger amounts of interlaminar failure. These trends have been observed for the three jet diameters being considered. For example, Fig. 2 is a typical impact site for a 4.5 mm jet and shows a small amount of matrix removal, but the delamination, which is extensive, takes the form of an inner disc, G, and a separate annulus of

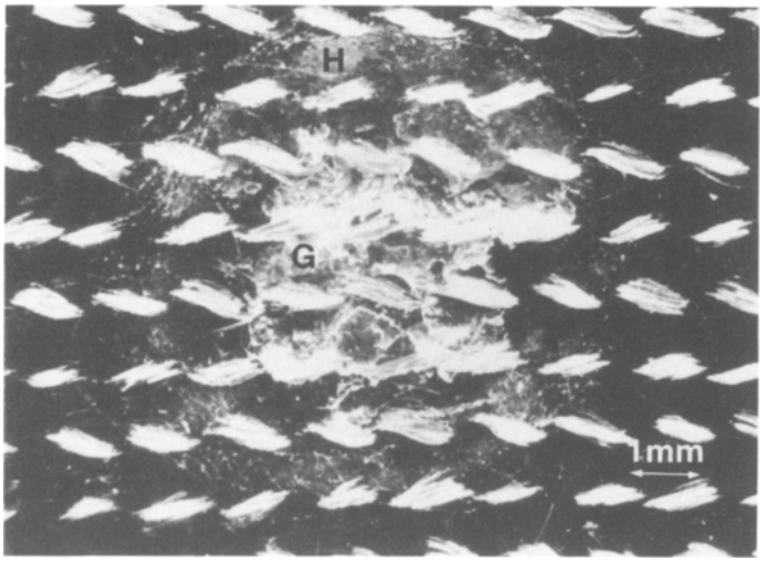


*Figure 2* Damage due to impact by a 600 m sec$^{-1}$ 4.5 mm diameter jet at normal incidence.

damage, H. The fact that the subsurface damage is split into two distinct regions (one inside and one outside the impacted zone) suggests that two damage mechanisms are operative. For the other jets these areas overlap. The cause of this phenomenon is not completely clear, but a number of possible mechanisms are discussed by Gorham and Field [6].

### 4.1. Quantitative damage assessment

To facilitate comparison between various experimental conditions, impact damage was assessed quantitatively by measuring the area of three visible types of damage: (a) rear surface spallation (only occurred for 4.5 mm jets), (b) surface material removal, and (c) interlaminar failure beneath the impact surface. This last type of damage is a close approximation to the total damage visible from the front surface.

Estimating damage by measuring mass loss was not employed as conditions were much less severe than would be necessary to produce appreciable mass loss for a single impact but they do produce significant degradation of material properties.

Fig. 3a, b and c shows how the areas of the different damage types vary with impact velocity for the three jet sizes considered. Each graph shows a damage threshold within a small velocity band, occurring at higher velocity for smaller jets. Above this threshold, damage increases very rapidly with increasing velocity. Over the range of velocities considered it was not possible to derive a meaningful value of the velocity exponent, $n$, in a relation of the form $A \propto (V - V_c)^n$, where $A$ is a damage area and $V_c$ is a critical velocity.

Rear surface spalling was only observed after impact by 4.5 mm jets and at velocities $\gtrsim$ 500 m sec$^{-1}$. The criterion for spall formation is that the magnitude of the tensile stress-wave formed when the main compressive wave reflects off the rear surface of the sample must exceed the interlaminar tensile failure stress at that strain rate. This means that spallation depends on the magnitude of the initial stress-pulse and on both the geometric and dispersive attenuation characteristics of the system. The samples under investigation are not thin and therefore the attenuation of the stress-pulse is high. The duration of the pulse depends on the jet radius and therefore the pulse duration for the 4.5 mm jet is 2 and 3 times as great as those for the 3 and 1.5 mm jets. Tauchert [8] finds that the attenuation coefficient $\beta$ (defined by the wave amplitude decay rate, $\exp(-\beta x)$, $x$ is distance travelled) for waves propagated in similar composite materials varies approximately parabolically with frequency. Therefore, a short duration pulse, containing a greater proportion of its energy in higher frequency Fourier components, suffers much greater attenuation than a long duration pulse. The area of contact of the jet also determines how important geometric attenuation (i.e. $1/r^2$) becomes. For a large jet the contact diameter is comparable with the sample thickness, resulting in a wave front that is more nearly planar at the rear surface.

These factors contribute to an overall attenu-

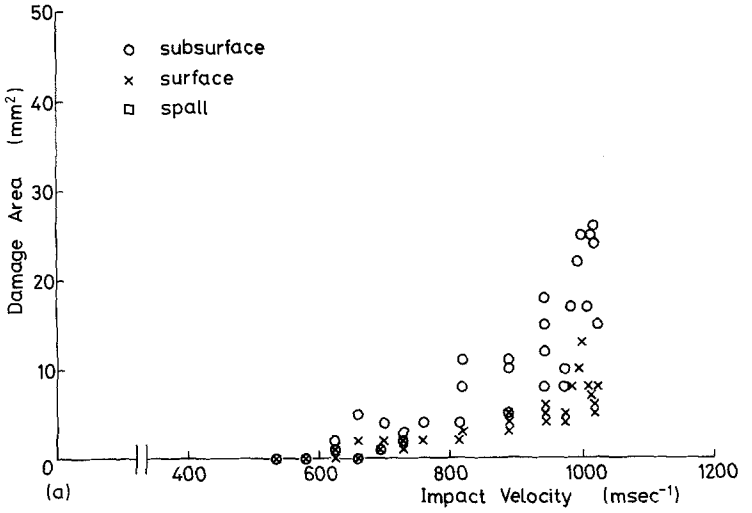


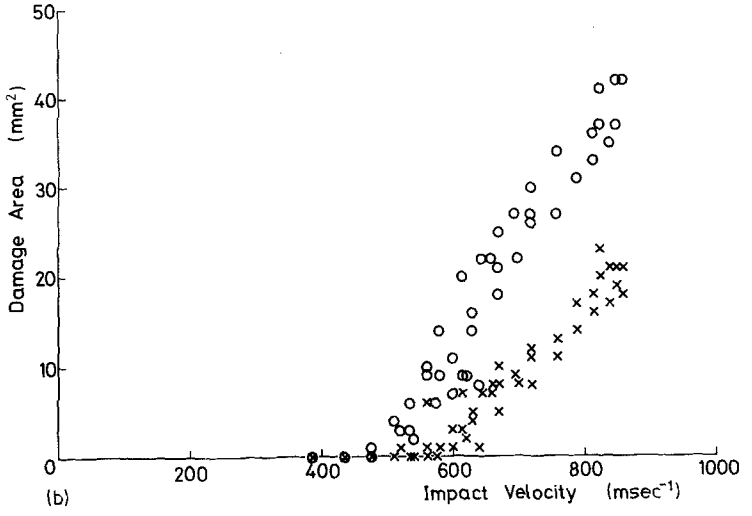


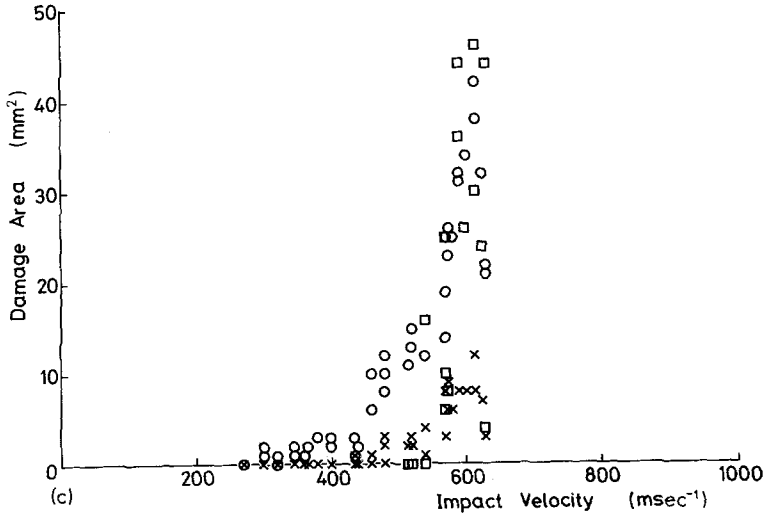


*Figure 3* Variation of damage areas with impact velocity for various jet diameters: (a) 1.5 mm; (b) 3.0 mm; and (c) 4.5 mm. Key for figures in this paper: ○ subsurface damage, × surface damage and ▲ spallation.

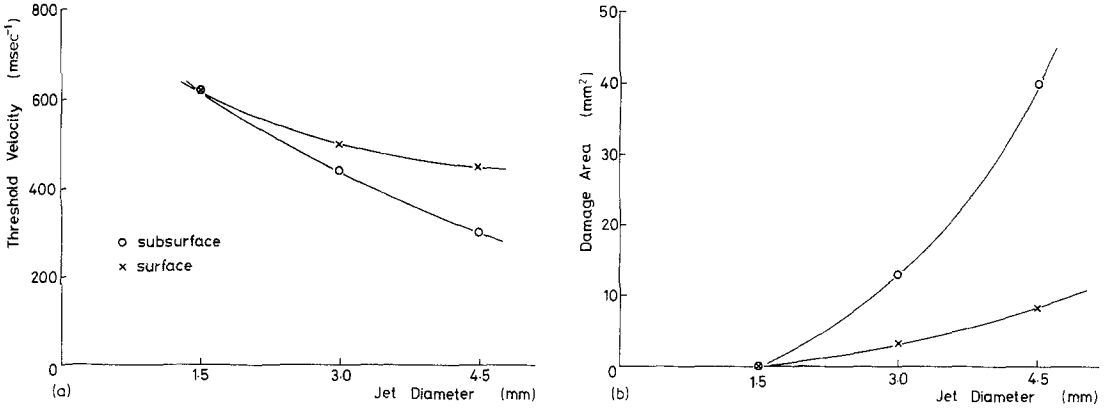


*Figure 4* Effect of jet size (nozzle diameter) on impact damage on the radome: (a) threshold velocity as a function of jet diameter, and (b) damage area as a function of jet diameter for a constant impact velocity of 600 m sec$^{-1}$.

ation factor which is less for the 4.5 mm jets than for the smaller diameters. The sample, being comparatively thick, attenuates the pulses to such an extent that only for the 4.5 mm jet is the spallation criterion satisfied in the range of velocities considered.

Fig. 4a shows how the threshold velocities for surface and subsurface damage change with jet diameter. More striking is how the damage rises rapidly with increasing jet size at a given velocity. Fig. 4b shows this variation for impacts at 600 m sec$^{-1}$. At this velocity no damage is visible for the smallest jet, while for the largest jet extensive ($\sim 40$ mm$^2$) subsurface damage occurs. The damage accelerates with jet size, even though the impact pressures are similar, and this effect is largely due to the impact duration. This evidence suggests that the damage suffered by the component under practical rain erosion will be strongly influenced by the few encounters with the largest drops present in the rain field. This is a justification for considering damage caused by jets whose equivalent drop sizes are quite large.

## 5. Oblique impact results

The dependence of the damage area on the angle of impact has been investigated for various velocities and jet sizes. Fig. 5 shows the variation of damage area with impact angle, $\alpha$, (the angle between the impacting jet and a normal to the surface) at four representative velocities for one jet diameter (3 mm), where each point represents the mean of at least four impacts. The form of the dependence is similar for the other jet sizes and velocities; Fig. 6 shows the results for the 1.5 mm jets, where the greater scatter is due to each point representing only one impact.

These figures show interesting features. Initially, for small angles of obliqueness, the damage falls off with increasing angle, passes through a minimum but increases to a maximum where damage is greater than that caused by normal impact. The angle of maximum damage increases with jet velocity.

A "rule of thumb" for isotropic materials is that the amount of damage caused by oblique liquid impact is the same as that produced by normal impact with a velocity equal to the normal velocity component of the obliquely impacting liquid, i.e. $V \cos \alpha$. Fig. 7 shows the sketched lines for angular behaviour of the subsurface damage from Fig. 5 (solid lines). Also shown is the behaviour that would be observed if the damage were dependent on $V \cos \alpha$ only (dashed lines, calculated from the normal impact data of Fig. 3b). The $V \cos \alpha$ assumption predicts that damage will fall monotonically with angle, but the observed behaviour differs from this in two important ways. Firstly, for slightly off-normal impacts the damage is much greater than expected and is appreciably greater than for normal impact. Secondly, the damage falls much more slowly with angle for highly oblique impacts and therefore the threshold angle for damage is larger than expected.

Fig. 8a and b shows damage sites for impacts by 3 mm jets for incidence angles of 15° and 50°. The scale of the photographs and the impact velocities (815 m sec$^{-1}$) are the same as those for Fig. 1a. The subsurface damage is greatly extended "downstream" of the jet and fibre breakage is very noticeable.

The explanation put forward for this phenomenon by Gorham and Field [9] is that the lateral jetting from beneath the impacting liquid is

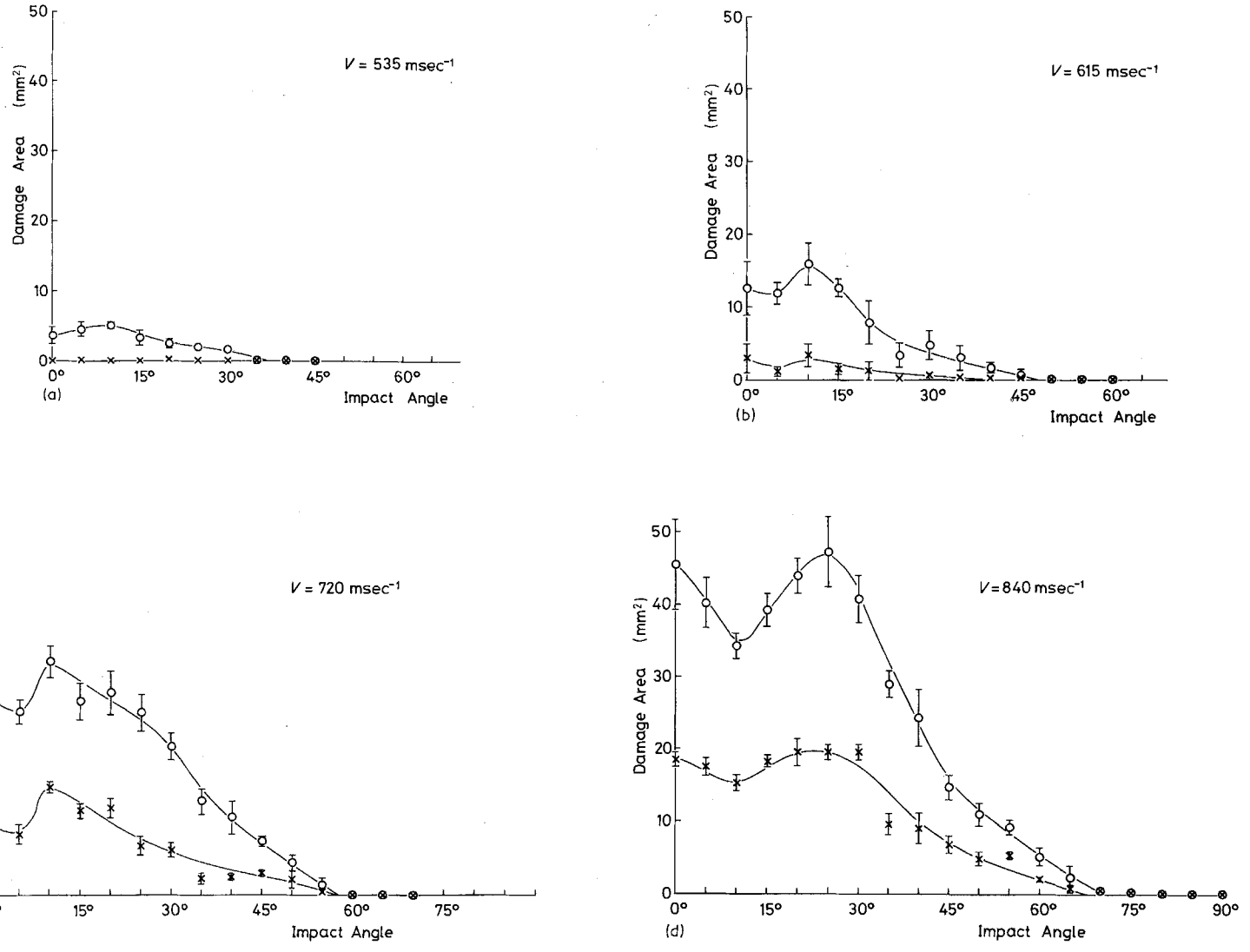


*Figure 5* Variation of damage areas with impact angle, $\alpha$, for impacts by 3 mm jets for impact velocities of: (a) 535 m sec$^{-1}$, (b) 615 m sec$^{-1}$, (c) 720 m sec$^{-1}$, and (d) 840 m sec$^{-1}$.

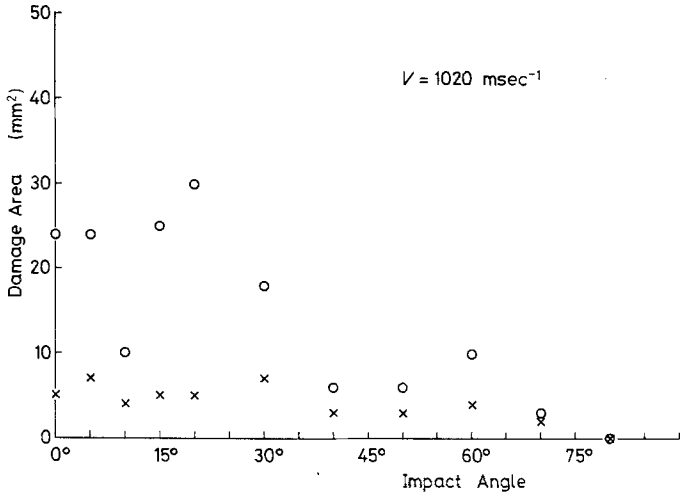


*Figure 6* Variation of damage areas with impact angle, $\alpha$, for impacts by 1.5 mm jets for an impact velocity of 1020 m sec$^{-1}$.

greatly enhanced in the downstream direction. Provided sufficient penetration has occurred, jetting between laminations spreads the interlaminar failure region downstream, a damage mode which only occurs for normal impact at very high velocities or after multiple impact. However, the enhancement of lateral jetting velocities does not become appreciable until a certain degree of obliqueness is reached, which means that the damage initially falls with angle before rising to its maximum value. This type of interlaminar failure is especially noticeable for multiple impact and will be discussed in the next section.

Fig. 8b shows a damage site at an angle of incidence near the critical angle for damage. Subsurface damage is not extensive because insufficient penetration has occurred for gross interlaminar failure. A noteworthy feature is the slight surface roughening upstream, R, which is typical of damage caused by jets impacting near the threshold velocity or angle for macroscopic damage. The roughening will be discussed in Section 7.

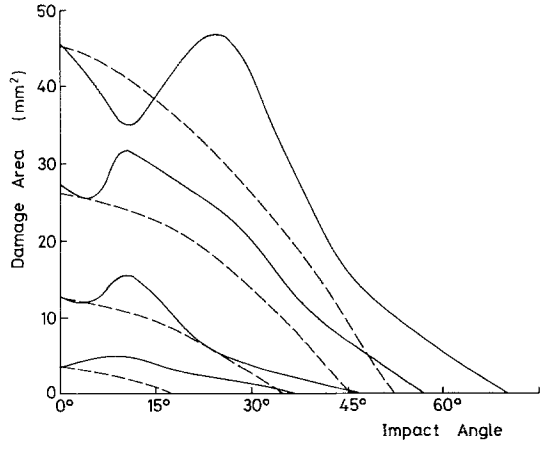


*Figure 7* Comparison between observed (solid lines) and predicted (dotted lines) behaviour using the $V\cos\alpha$ assumption for oblique impact by 3 mm jets.

## 6. Multiple impact

Damage caused by two or three impacts on the same site has been found to be very extensive. As shown in the previous section, the first impact at a sufficiently high velocity causes matrix removal, exposure of fibre bundles and interlaminar failure. The extent of material removal by a single impact is therefore largely dependent on the matrix properties, but for the second impact the properties of the now fully exposed fibre bundles are relevant. In many cases all the bundles intersecting the central damage zone are severed by the second impact, exposing further laminations and leading to increased penetration by subsequent impacts. The central damage region is greatly increased in size by the removal of matrix from around the edges, already weakened by the first impact (see Fig. 1c). The most noticeable effect is the increase in interlaminar failure caused by the lateral jetting between reinforcement layers. If an interlaminar fissure contains liquid before the impact, the $\rho CV$ "water hammer" pressure is propagated throughout the fissure resulting in large-scale damage at some distance from the impact region. It was found that if the samples were dried prior to the second impact, damage, while still extensive, was less than for still wet specimens. In practice, of course, the eroding component will not be dried between impacts. After multiple impact interlaminar failure is very extensive and gross lifting

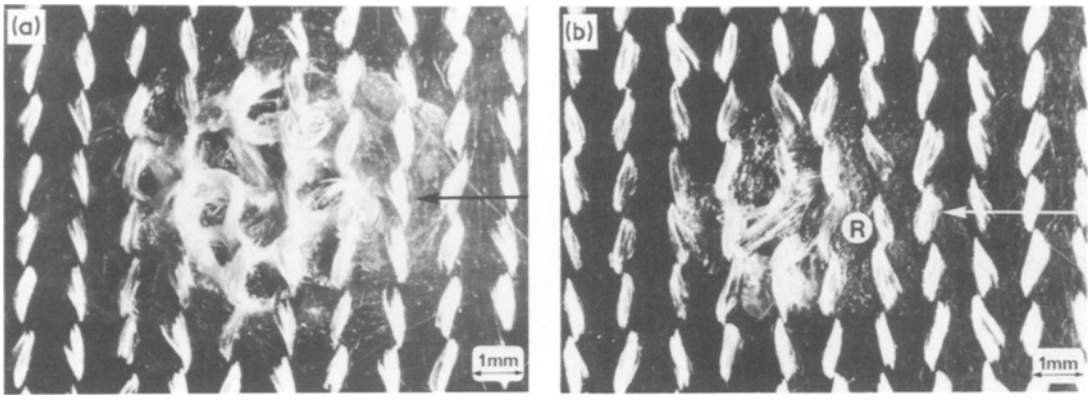


*Figure 8* Damage sites due to impact by 815 m sec$^{-1}$, 3 mm diameter jets. The impact angles, $\alpha$, are (a) 15° and (b) 50°. The arrows denote the direction of impact.

of the surface around the impact zone is observed. This "hydraulic" effect has been proposed as a mechanism for rivet head damage by Field, Camus and Gorham [10]. The first few impacts on the rivet lift its edges slightly and water can then penetrate between the rivet head and the rivetted sheet. Subsequent impacts cause large deformations of the rivet by this hydraulic effect. A similar process may occur once a crack is produced and subsequent impacts pressurize any liquid trapped in it.

For oblique impact one observes greater extension in the downstream delamination after successive impacts, and for near normal incidence (10° to 30°) the damage peak is accentuated because of easier interlaminar jetting. Fig. 9 shows the variations of subsurface damage area with impact angle for one and two impacts. 3 mm jets at 720 m sec$^{-1}$ were used. The peak of damage for two impacts is very much higher than for one impact and is at a larger angle of obliquity. The threshold angle for visible damage is slightly increased showing that the second impact extends invisible damage produced by the first. The damage area is approximately doubled by the second impact at most angles and the total volume of damaged material is increased by a factor of ~ 3 to 4.

## 7. Multiple subcritical impact

In practical situations materials are rarely used in conditions where visible erosion damage occurs after only a few impacts, and the present investigations have shown that severe damage may result from repeated impacts at angles or velocities which would not show macroscopic damage after only a few impacts.

Fig. 10a is a site which has been impacted at normal incidence ten times by 3 mm jets with a velocity of 430 m sec$^{-1}$. After five impacts only a slight surface roughening was observed, but then

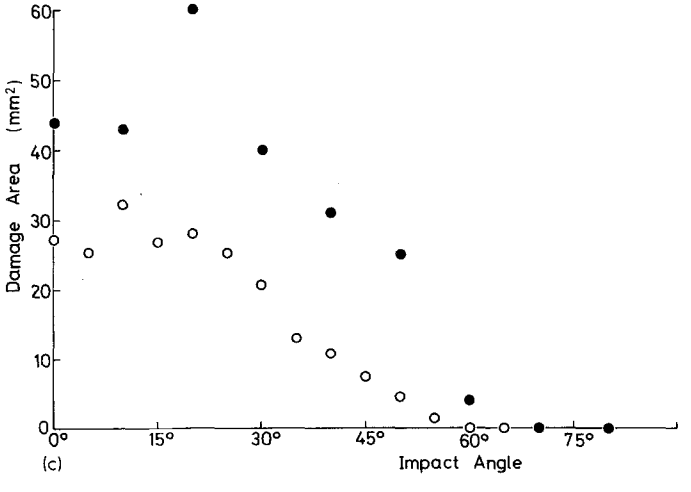


*Figure 9* Damage areas produced by the impact of 720 m sec$^{-1}$, 3 mm jets as a function of impact angle for: ○ one impact and ● two impacts.

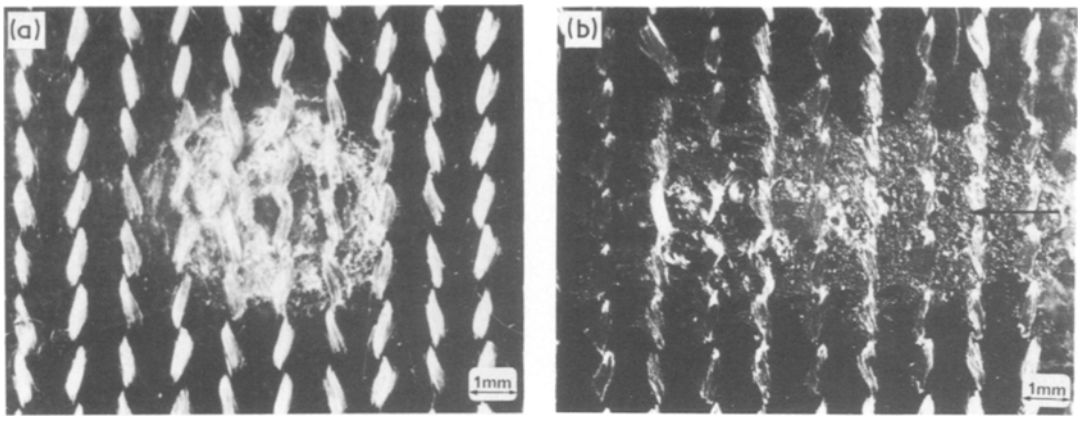


*Figure 10* Damage produced by ten "subcritical" impacts by 3 mm jets: (a) at normal incidence with an impact velocity of 430 m sec$^{-1}$, and (b) at an angle of $\alpha = 79°$ at 760 m sec$^{-1}$; the arrow denotes the direction of impact.

damage rapidly accelerated leaving a ring of damage where matrix removal had occurred around a central undamaged region.

Under operating conditions the radome makes a maximum angle of 11° to the relative airflow. Fig. 10b is a sample impacted ten times by a 3 mm jet at 760 m sec$^{-1}$ at this angle (an impact angle of 79° which is well above the critical angle for single-impact damage, ~65°). Widespread surface roughening is observed. Although a single impact does not produce noticeable damage, lateral jetting velocities are high enough to erode surface discontinuities. Field [11] has shown that surface steps as small as 0.1 $\mu$m may be eroded by liquid impact. This form of roughening has been observed on a microscopic scale for both normal and oblique impacts under conditions which do not produce macroscopic damage. Fig. 8b is typical, where the upstream lateral jetting, too slow to do as much damage as downstream, has significantly roughened the surface. This roughening enhances erosion by subsequent impacts, leading to an accumulation of microscopic damage which may eventually result in macroscopic damage, as downstream of the jet in Fig. 10b where fibre bundles have been exposed by matrix removal.

Microscopic examination of the roughened surfaces suggests that surface irregularities on the specimen are the nucleation points. To demonstrate this some specimens were covered by a thin spray coat of cellulose paint which provides a smooth surface. After repeated impacts under the conditions described in this section no surface roughening of the paint occurred. The adhesion of the paint was relatively low and after several impacts debonding occurred, followed by eventual stripping. However, the experiment indicates that a smooth, well-adhering paint coat can greatly delay the formation of damage.

In summary, slow moving or highly oblique jets which do not produce visible damage, may, after repeated impact, lead to serious accumulative damage.

## 8. Conclusions

The impact properties of this radome material have been studied in detail for a variety of impact conditions. The amount of damage produced by the impacts has been quantified in terms of the visible area of damage, enabling comparisons to be made between impacts under differing conditions of jet size, velocity and angle.

The threshold velocities for damage have been found as a function of jet (hence rain-drop) diameter and indicate that the few impacts with the largest rain drops will control the initial stages of erosion.

A strong oblique impact anomaly is exhibited by this material: impacts at moderately oblique angles (10° to 30°) produce more damage than at normal incidence. This effect becomes more pronounced with subsequent impacts.

Multiple impact at velocities or angles which do not produce macroscopic damage for a single impact do produce an accumulation of microscopic damage which results in more serious deformations.

The impact properties of this material might appear to be rather poor. One or two near normal impacts can cause up to ~60 mm$^2$ of subsurface damage and repeated impacts under simulated flight conditions produce severe surface rough-

ening. However, there are a variety of reasons why this radome is flown safely.

(1) Concorde is only flown at supersonic speeds at altitudes at which rain is unlikely to occur (25 000 m).

(2) The specimens are not of production quality. Their surface condition was poor; the fibre reinforcement is at the matrix–air interface and the resin matrix surface has crazes and voids.

(3) Production radomes are coated with a tough layer of polyurethane paint. This layer behaves to a certain extent like a protective coating but more importantly, it gives a smooth finish which makes the initiation of damage by the interaction of fluid flow with small surface irregularities unlikely.

(4) The investigation has simulated extremely severe conditions, that is, the equivalent of impacts by large drops at high velocity and often at near normal incidence. Under such unrealistic conditions heavy damage is to be expected in a composite, as composites in general have poor rain erosion characteristics compared with other materials.

However, the results are relevant as they outline the fundamental failure mechanisms and the conditions under which they occur thereby allowing one to deduce certain design principles. The main points to emerge from this work are listed below.

(a) A component should have a smooth surface finish. Surface irregularities act as damage nucleation sites.

(b) Impact angles of 10° to 30° should be avoided as damage may be enhanced under some conditions.

(c) Damage falls rapidly with increasing impact angle for large angles, provided the specimen has a smooth surface. Therefore, large sweep-back is desirable.

(d) Impact by the largest expected drops must be considered as well as drops of average size since large drops produce disproportionately more damage than smaller ones and impacts by them can control the onset of erosion.

## Acknowledgements

We thank B. Ae. (Dynamics) Stevenage for providing the specimens and details of their construction. We also thank the Ministry of Defence (Procurement Executive) for financial support during the course of this work. One of us (MJM) thanks the Science Research Council and Churchill College, Cambridge.

## References

1. F. P. BOWDEN and J. H. BRUNTON, *Proc. Roy. Soc.* **A263** (1961) 433.
2. J. E. FIELD, D. A. GORHAM and D. G. RICKERBY, in "Erosion: Prevention and Useful Applications", edited by W. F. Adler, ASTM STP664 (American Society for Testing Metals, Ohio, 1979) p. 298.
3. J. E. FIELD, J.-J. CAMUS, D. A. GORHAM and D. G. RICKERBY, Proceedings of the 4th International Conference on Rain Erosion and Allied Phenomena, Meersburg, 1974 edited by A. A. Fyall and R. B. King (Royal Aircraft Establishment, Farnborough, UK, 1979).
4. W. G. REINECKE and G. D. WALDMAN, Proceedings of the 3rd International Conference on Rain Erosion and Allied Phenomena, RAE Farnborough, edited by A. A. Fyall and R. B. King, (Royal Aircraft Establishment, Farnborough, UK, 1970).
5. E. V. HARPER, G. W. GRUBE and I-DEE CHANG, *J. Fluid Mech.* **52** (1972) 565.
6. D. A. GORHAM and J. E. FIELD, *J. Phys. D: Appl. Phys.* **9** (1976) 1529.
7. F. P. BOWDEN and J. E. FIELD, *Proc. Roy. Soc. Lond.* **A282** (1964) 331.
8. T. R. TAUCHERT, *J. Composite Mater.* **5** (1971) 456.
9. D. A. GORHAM and J. E. FIELD, *Wear* **41** (1977) 213.
10. J. E. FIELD, J.-J. CAMUS and D. A. GORHAM, Proceedings of the 3rd International Conference on Rain Erosion and Allied Phenomena, RAE Farnborough, (1970) edited by A. A. Fyall and R. B. King, (Royal Aircraft Establishment, Farnborough, UK, 1970).
11. J. E. FIELD, Proceedings of the 2nd International Conference on Rain Erosion and Allied Phenomena, Meersburg, (1967) edited by A. A. Fyall and R. B. King, (Royal Aircraft Establishment, Farnborough, UK, 1967).

Received 24 October and accepted 21 November 1980.